Hurricane Wave Topography and Directional Wave Spectra in Near Real-Time

Edward J. Walsh
NASA/Goddard Space Flight Center, Code 614.6
Wallops Flight Facility, Wallops Island, VA 23337
phone: (303) 497-6357 fax: (303) 497-6181 email: edward.walsh@nasa.gov

C. Wayne Wright
NASA/Goddard Space Flight Center, Code 614.6
Wallops Flight Facility, Wallops Island, VA 23337
phone: (443) 783-3319 fax: (757) 824-1036 email: charles.w.wright@nasa.gov

Document Number: N0001407IP20002

LONG-TERM GOALS

Develop a simple parameterization for the directional wave spectrum in the vicinity of a hurricane.

OBJECTIVES

Develop and/or modify the real-time operating system and analysis techniques and programs of the NASA Scanning Radar Altimeter (SRA) to process the SRA wave topography data into directional wave spectra during hurricane flights. Upload the spectra and the topography onto a web site immediately post-flight to make them available to ONR investigators.

APPROACH

The SRA has a long heritage in measuring the energetic portion of the sea surface directional wave spectrum (Walsh et al. 1985; 1989; 1996, 2002; Wright et al. 2001). The wave spectra have been used to assess the output of the WaveWatch III numerical wave model (Moon et al., 2003; Fan et al., 2007). To obtain the directional wave spectrum, the energy in the encounter spectrum generated from the SRA wave topography must be doubled everywhere, the artifact lobes deleted, and the real lobes Doppler-corrected. Identifying the artifact lobes for deletion and partitioning the real spectral lobes into the various wave components has been a slow and labor-intensive process and efforts have been made toward eliminating operator decisions in that process to enable unattended operation.

WORK COMPLETED

After flying into hurricanes aboard a NOAA aircraft for eight seasons (1998-2005) the NASA SRA experienced significant hardware problems and was decommissioned. NOAA awarded a contract to ProSensing (prosensing.com) to build an operational SRA. It should be shipped to the NOAA Aircraft Operations Center in Tampa by 15 October 2007. The NASA-developed software and analysis techniques have been tailored to the new NOAA SRA hardware and system characteristics to enable data processing and transmitting final data products to the National Hurricane Center (NHC) during the flights to provide an enduring legacy to ONR investigators and the nation.

Report Documentation Page						*Form Approved* *OMB No. 0704-0188*
Public reporting burden for the collection of information is estimated to average 1 hour per response, including the time for reviewing instructions, searching existing data sources, gathering and maintaining the data needed, and completing and reviewing the collection of information. Send comments regarding this burden estimate or any other aspect of this collection of information, including suggestions for reducing this burden, to Washington Headquarters Services, Directorate for Information Operations and Reports, 1215 Jefferson Davis Highway, Suite 1204, Arlington VA 22202-4302. Respondents should be aware that notwithstanding any other provision of law, no person shall be subject to a penalty for failing to comply with a collection of information if it does not display a currently valid OMB control number.						
1. REPORT DATE **30 SEP 2007**		2. REPORT TYPE **Annual**				3. DATES COVERED **00-00-2007 to 00-00-2007**
4. TITLE AND SUBTITLE **Hurricane Wave Topography And Directional Wave Spectra In Near Real-Time**						5a. CONTRACT NUMBER
						5b. GRANT NUMBER
						5c. PROGRAM ELEMENT NUMBER
6. AUTHOR(S)						5d. PROJECT NUMBER
						5e. TASK NUMBER
						5f. WORK UNIT NUMBER
7. PERFORMING ORGANIZATION NAME(S) AND ADDRESS(ES) **NASA/Goddard Space Flight Center, Code 614.6,Wallops Flight Facility,Wallops Island,VA,23337**						8. PERFORMING ORGANIZATION REPORT NUMBER
9. SPONSORING/MONITORING AGENCY NAME(S) AND ADDRESS(ES)						10. SPONSOR/MONITOR’S ACRONYM(S)
						11. SPONSOR/MONITOR’S REPORT NUMBER(S)
12. DISTRIBUTION/AVAILABILITY STATEMENT **Approved for public release; distribution unlimited**						
13. SUPPLEMENTARY NOTES **code 1 only**						
14. ABSTRACT **Develop a simple parameterization for the directional wave spectrum in the vicinity of a hurricane.**						
15. SUBJECT TERMS						
16. SECURITY CLASSIFICATION OF:			17. LIMITATION OF ABSTRACT	18. NUMBER OF PAGES	19a. NAME OF RESPONSIBLE PERSON	
a. REPORT **unclassified**	b. ABSTRACT **unclassified**	c. THIS PAGE **unclassified**	**Same as Report (SAR)**	**11**		

Standard Form 298 (Rev. 8-98)
Prescribed by ANSI Std Z39-18

RESULTS

Figure 1 shows the output of the initial SRA display software which has been installed and tested on an NHC computer using data acquired during a flight into Hurricane Humberto on 24 September 2001. Each time the program is run, it reads in all the SRA data files sent from the aircraft and accumulated in a directory in the NHC computer, finds the maximum SWH and automatically generates a plan view of the aircraft track through the hurricane, color coding the wave height red at the 16', 20', 24', 28', 32', or 36' level, depending on the maximum level the wave height exceeds. So unless the waves are lower than 16', the display will always contain all the colors (green, black, blue, red). Future programs will display entire directional spectra.

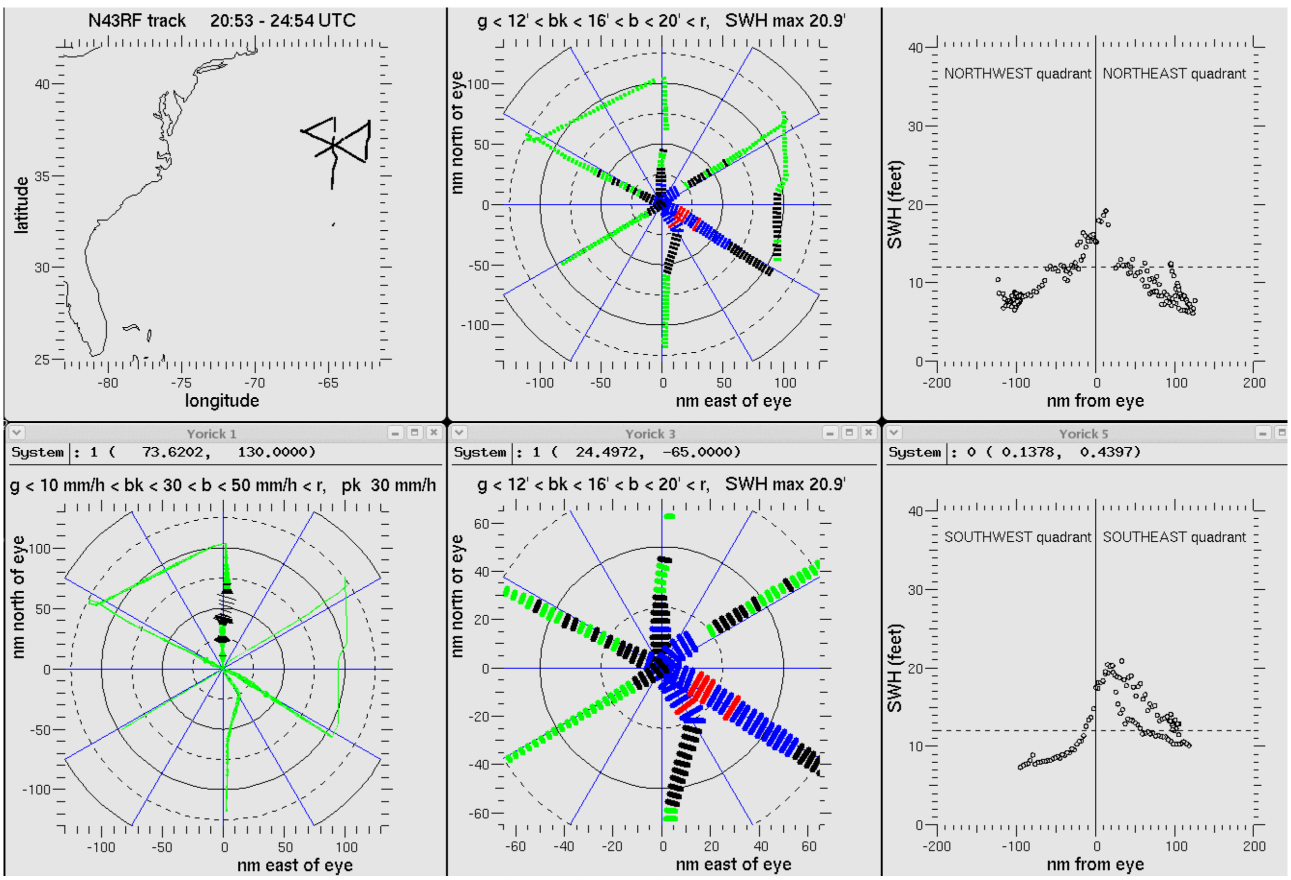

Figure 1. Display for SRA software installed and tested on National Hurricane Center computer.

The 2006 annual report (Document Number N0001406IP20037) included an analysis focused on quantifying distortions in the measured wave spectra produced by variations in the power backscattered by the sea surface. The antenna of the new NOAA SRA forms its beams digitally instead of scanning a lens-generated beam mechanically as the NASA system did, but both two-way beamwidths are 1° and the effective swath is between 22° off-nadir to the left of the aircraft track, through nadir, to 22° off-nadir to the right. The solid, parallel lines in Figure 2 (from the 2006 report) show the 0.9 m half-power width bounds of the SRA pulse approaching the sea surface from 1500 m

altitude. The horizontal sinusoidal curve represents an ocean wave of 50 m length and 1.67 m crest-to-trough height. The solid line orthogonal to the transmitted pulse indicates the antenna boresight and the dashed and dotted lines parallel to it indicate the half-power and 0.1 power limits of the 1° two-way antenna pattern, modeled as Gaussian.

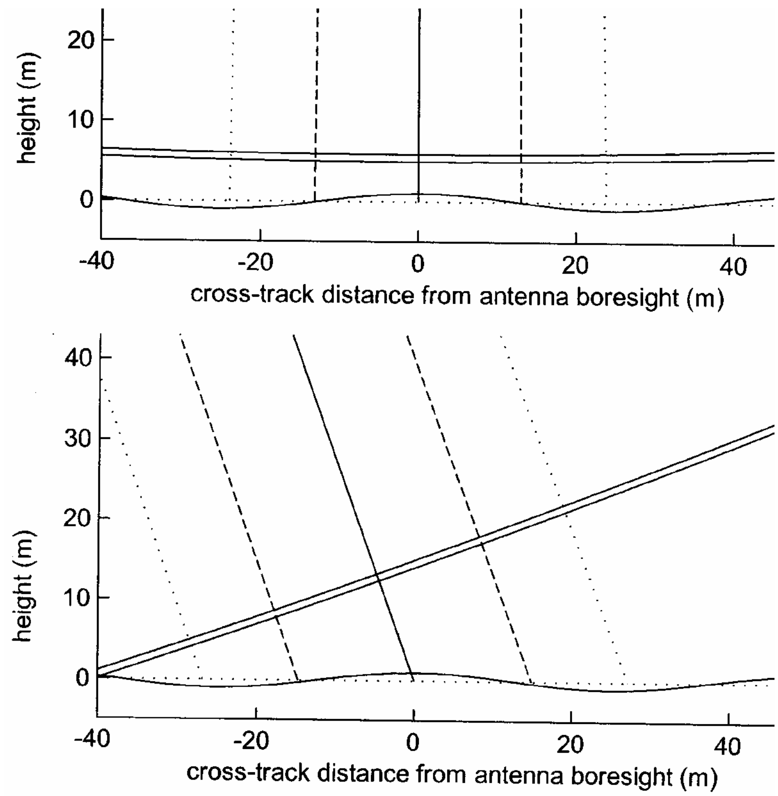

Figure 2. Nadir and off-nadir geometry for the SRA pulse transmitted from 1500 m height interacting with an ocean wave of 50 m length.

It is apparent that the centroid of the backscattered power for the pulse approaching the nadir point in the top panel will determine a range greater than that to the wave crest at the boresight because the half-power width of the antenna pattern extends to mean sea level. The reverse would be true for a trough at the boresight. This spatial filtering by the antenna footprint reduces the measured wave height at nadir.

In the bottom panel of Figure 2 the antenna boresight is 20° off-nadir. The wave crest at the boresight makes the local incidence angle 20° there, but places the maximum ±6° slopes of the 50 m length wave at the antenna half-power points. The local incidence angle is 26.5° at the off-nadir antenna half-power limit and 13.5° at the near-nadir limit. The smaller local incidence angle on the near-nadir side of the wave crest will increase the backscattered power and shift its centroid to shorter range. Ascribing the shorter range to the antenna boresight angle will increase the apparent height of the wave crest. If a wave trough were at the antenna boresight, the local incidence angle would be 15.5° at the off-nadir half-power antenna limit and 25.5° at the near-nadir limit. The lower local incidence angle

on the off-nadir side of the trough would increase the backscattered power and shift the power centroid to longer range, erroneously indicating a deeper wave trough at the antenna boresight.

To be able to model and correct these distortions it is necessary to know the variation of the backscattered power with incidence angle, which is a function of the sea surface mean square slope (mss), principally determined by the small scale roughness. The Plant (1982) theoretical maximum limit on mss at high wind speed is 0.080. The backscattered power is generally assumed to fall off in a Gaussian fashion near nadir with the falloff rate being determined by the reciprocal of the mss (Walsh et al. 2008).

When the log of the backscattered power is plotted versus the square of the incidence angle tangent, the Gaussian assumption produces a straight line. But Figure 3 shows SRA data indicating that its measurements extend far enough off nadir that the strictly Gaussian assumption is not valid. The data are better fit with curves of the form

$$ln\, P(S) = -A S^2 + B S^4 \qquad (1)$$

where S is the incidence angle tangent. In the Gaussian assumption, $B = 0$. The B term moderates the falloff of the backscattered power and reduces the distortion in the spectral measurements.

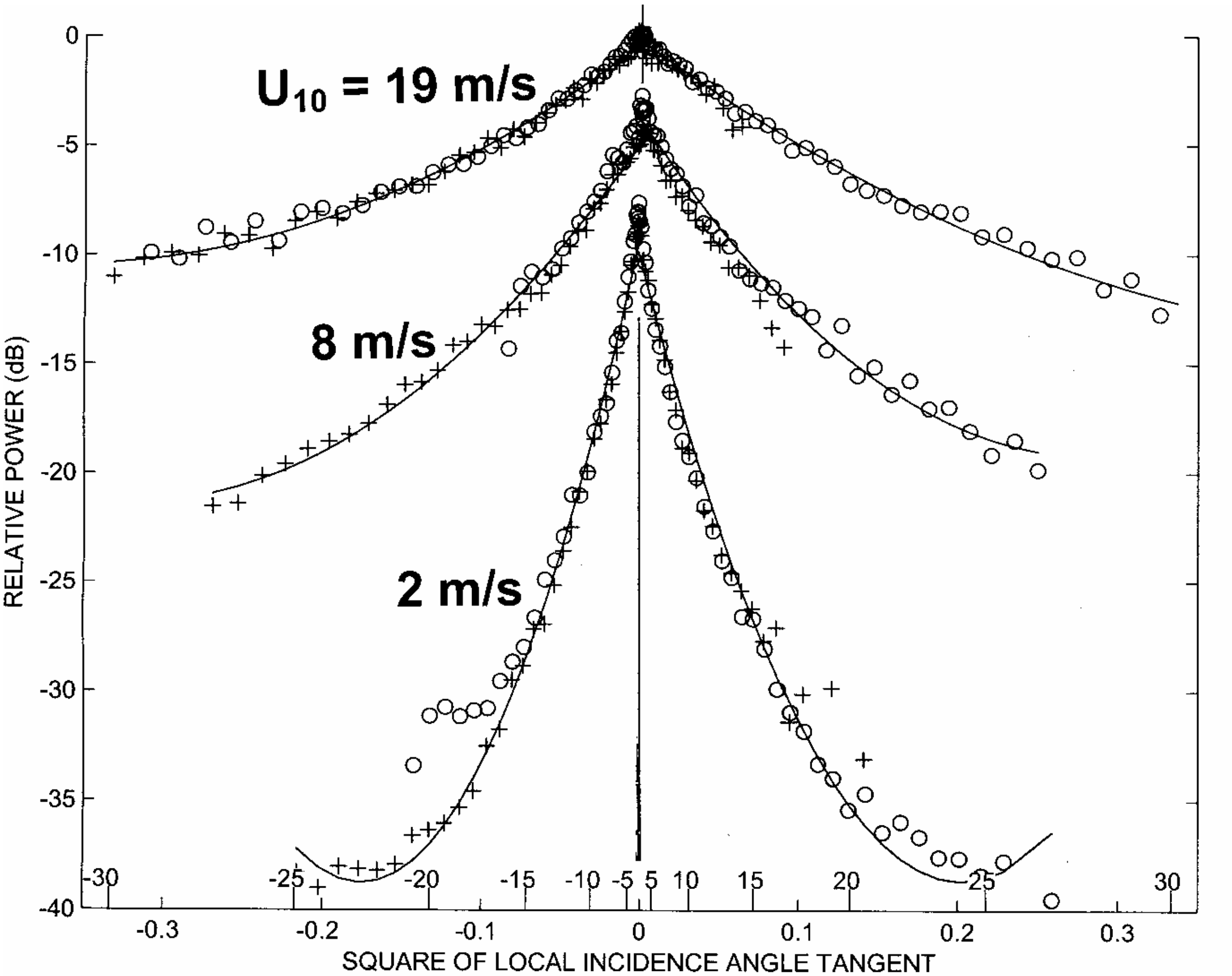

Figure 3. Backscattered power variation for the SRA scan plane within ±7.5° of the upwind-downwind direction with positive angles indicating the downwind direction. Circles indicate data for which the right side of the SRA scan plane was oriented downwind and + symbols indicate the data for which the right side of the scan plane was oriented upwind. The data for 8 m s^{-1} were shifted down by 10 dB and the data for 2 m s^{-1} were shifted down by 15 dB to prevent overlap. The second-order curves on the right side were least-squares fitted to the circles and the curves on the left side were least-squares fitted to the + signs.

There were several problems in trying to use SRA hurricane data to investigate the backscattered power variation with incidence angle. At the generally high altitudes of the hurricane flights the SRA signal level was low, the footprint was large, and data were not available over a wide variety of azimuths to do a comprehensive analysis. The SRA data used were acquired at low altitude in the Southern Ocean with complete azimuthal coverage over a wide range of sea states (up to 9 m wave height) and wind speeds, though less than hurricane force (Walsh et al. 2008). Figure 4 shows the measurement geometry. Data were acquired with the aircraft in a 7° roll attitude while it turned azimuthally through 810°. The small antenna footprint (4 m) allowed computation of the along- and

cross-track components of sea surface slope at each measurement point to compute local incidence angles for each backscattered power value.

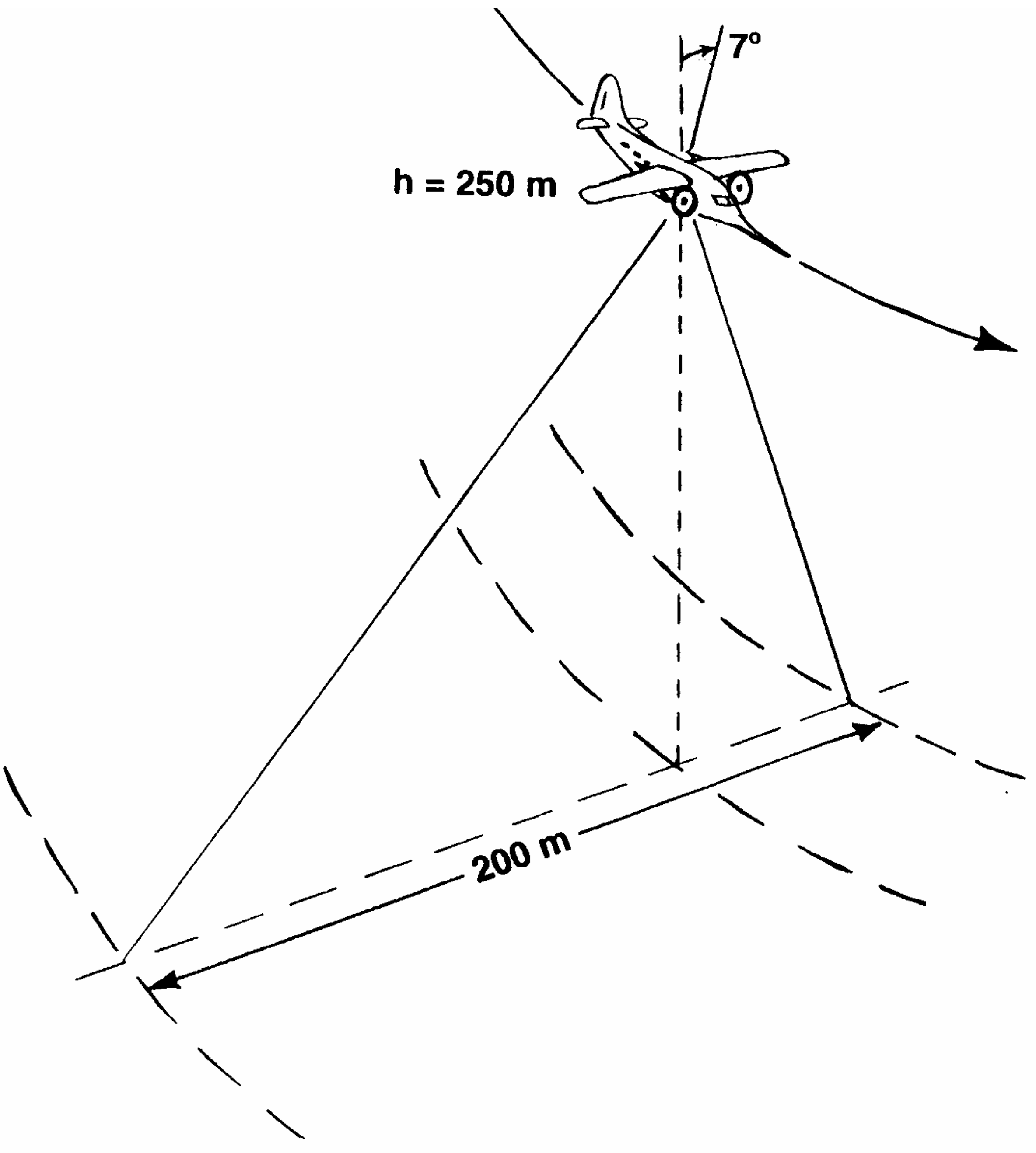

Figure 4. Measurement geometry for data acquired at 250 m altitude while the aircraft was in a -7° roll attitude.

Figure 5 shows a representative data segment. Acquiring data at all azimuths relative to the wind direction required spending relatively little time in any particular azimuth interval. The slopes associated with the few dominant waves observed in a particular azimuth interval would not be statistically representative of the overall slope distribution of the sea state and would not even be the same at all off-nadir incidence angles in any particular azimuth interval. The result would be a significant misbinning of the rapidly fluctuating backscattered power data with respect to the actual incidence angles and a corruption of the resulting distributions. The high quality of the surface slope data displayed in Figure 5 suggest that sea surface slopes on scales too small to be resolved by the SRA wave topography measurements would be small enough that their distribution could be considered statistically identical at all incidence angle and azimuth intervals.

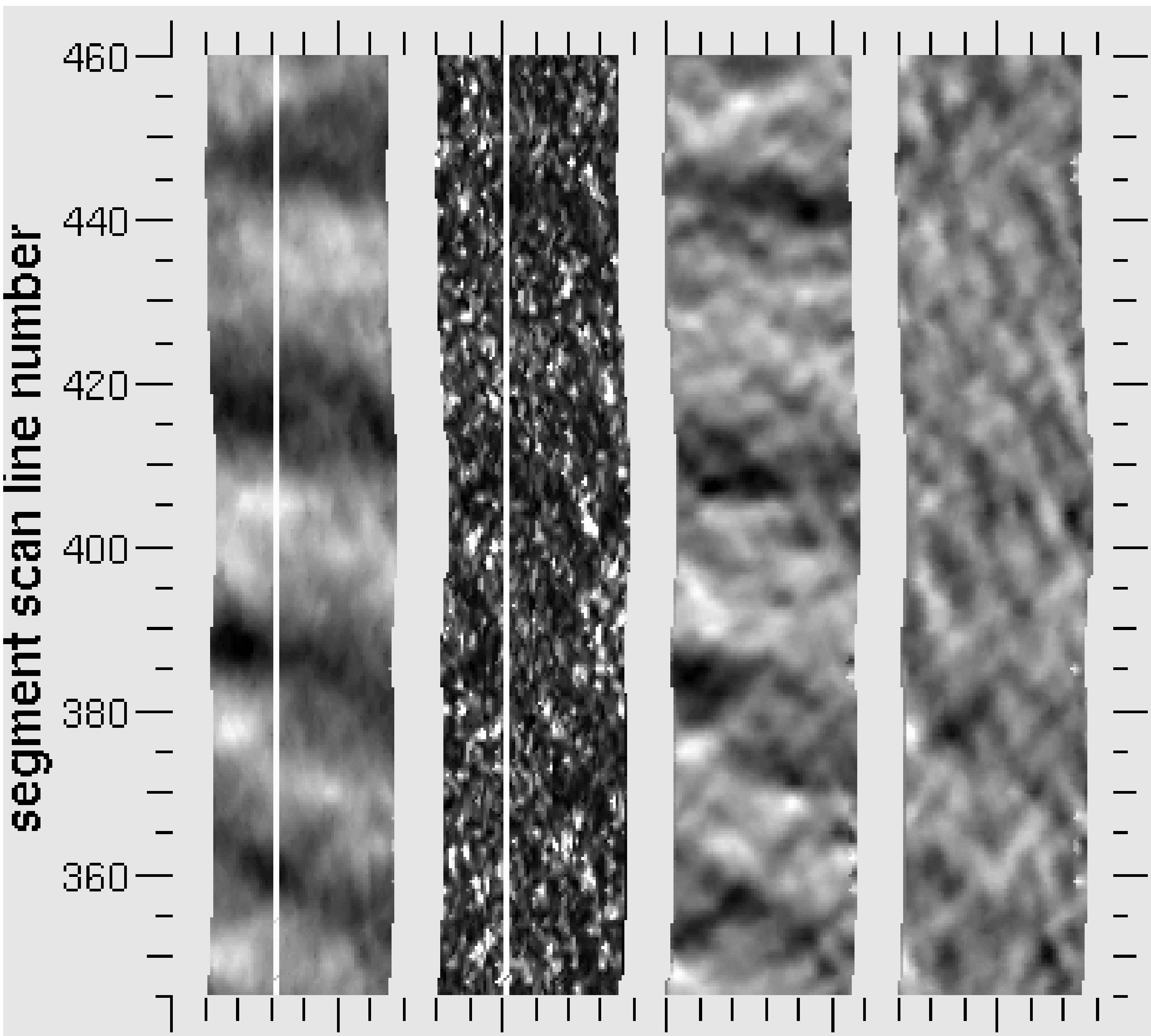

Figure 5. SRA wave topography (left panel) and backscattered power with the average cross-track power variation removed (second panel). The white line indicates the nadir point. The third and fourth panels are the along-track and cross-track sea surface slopes, respectively.

The circles in Figure 6 show the quadratic (*B*) coefficient plotted against the linear (*A*) coefficient (equation 1) for all the second-order fits to the SRA data such as shown by the curves in Figure 3. The straight line in Figure 6 was least-squares fitted to the logarithms of the *B* and *A* coefficients for all the data. Its equation is the power law

$$B = 0.4182\ A^{1.434} \tag{2}$$

The straight line with dots was least-squares fitted to the logarithms of the *B* and *A* coefficients for all the data except the lightest wind-speed day (60<*A*<100), resulting in

$$B = 0.5676\ A^{1.332} \tag{3}$$

The dashed curve is actually a straight line (appearing curved due to the log-log axes in Figure 6) that was least-squares fitted to the *B* and *A* coefficients for all the data except the lightest wind-speed day. Its equation is

$$B = -9.84 + 2.066A\ . \tag{4}$$

The dashed and solid curves indicate a very similar dependence of *B* on *A* for values of *A* less than 40. If the cluster of data for the 2 m s^{-1} wind speed day (60<*A*<100) were included in the linear dependence curve fit (4), the fit to the main body of data would have degraded significantly. The equation of the dotted line, least-squares fitted to the log of the three Ku-band values (+ symbols) from the Voronovich and Zavorotny (2001) theoretical analysis is

$$B = 0.4194\,A^{1.327} \tag{5}$$

This analysis indicates that the non-Gaussian characteristic of the scattering increases as the mss increases. Figure 6 suggests the possibility that there may be a global model to characterize Ka-band radar backscatter from the sea surface within 25° of nadir and that the quadratic (*B*) coefficient is uniquely related to the linear (*A*) coefficient. Except for the lightest wind day, there was considerable overlap in the *A* and *B* coefficients from day to day because they varied significantly azimuthally. But the scatter for any given day spread the coefficients along the general power law representing the entire dataset. This is important because it suggests that for a particular value of the *A* coefficient, the same *B* coefficient will be associated with it whether the *A* coefficient corresponded to the crosswind direction at a high wind speed, or to the upwind direction at a lower wind speed, or to an intermediate wind speed at an intermediate direction relative to the wind.

The Voronovich and Zavorotny (2001) Ku-band theoretical analysis, which used only Gaussian slope statistics but included diffraction, produced almost the same power law relationship between *A* and *B* as the SRA Ka-band observations. Further investigation is needed to determine whether the offset between the Ku-band curve fit to their theoretical results and the Ka-band data is due to a contribution of non-Gaussian slope statistics, or to the frequency difference, or to problems in the theory and/or measurements. But what it suggests is that whether the non-Gaussian nature of the scattering is caused by non-Gaussian slope statistics, or Gaussian slope statistics and diffraction, or some combination of

the two, the linear coefficient, *A*, is sufficient to determine the characteristics of the backscatter since the quadratic coefficient, *B*, can be related to it.

It should be emphasized that the relationship between *A* and *B* was not obtained using off-nadir angles, but local incidence angles which took into account the slopes of waves whose wavelengths were longer than about 16 to 25 m. Equation (2) resulting from this analysis can be used in the correction of SRA hurricane spectra but it may have more general application. Computing local incidence angles is not possible for satellite remote sensors. But their measurements, binned by off-nadir angle, are generally averaged over areas large enough that long-wave slopes can be assumed to be statistically represented at all incidence angles. This simple model might prove very useful for predicting the performance of remote sensors that operate within 25° of nadir.

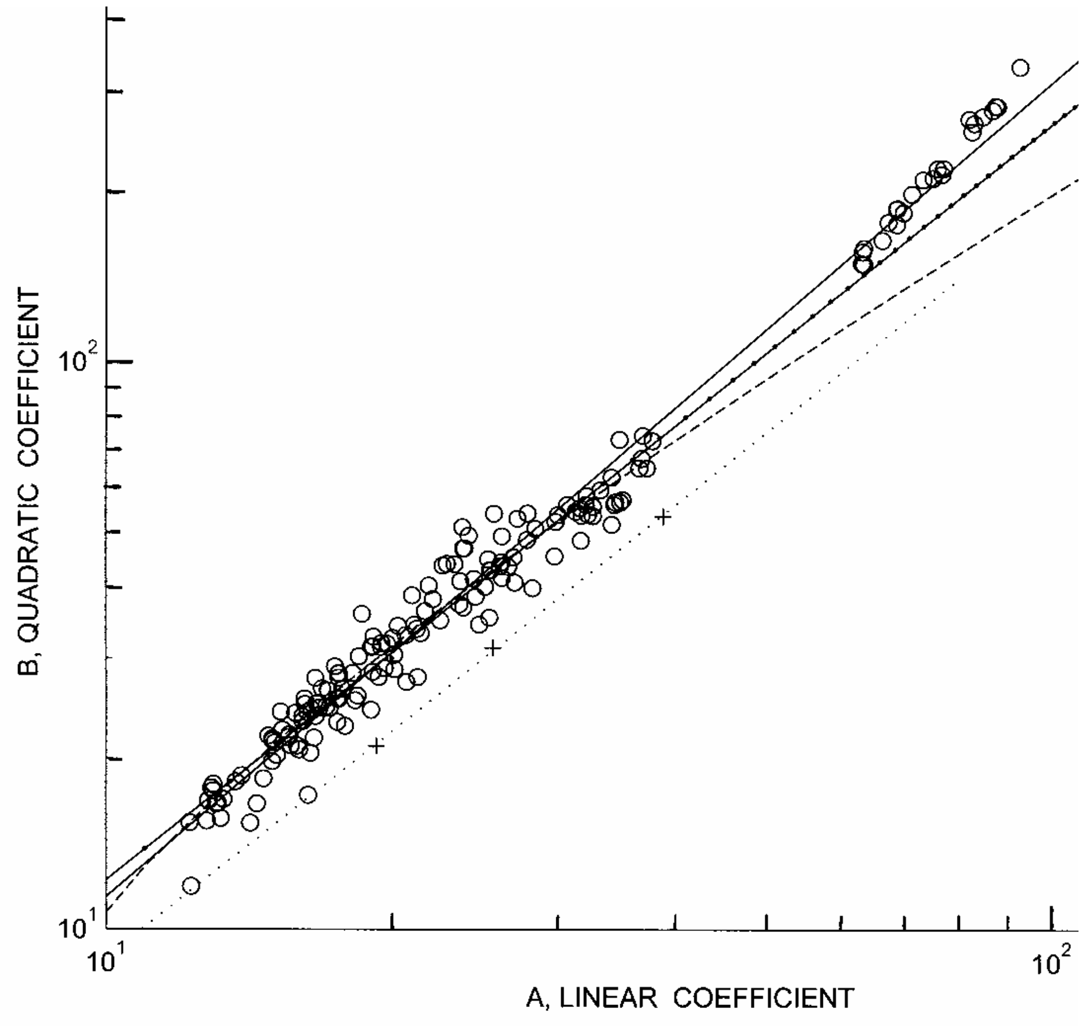

Figure 6. Quadratic (B) coefficient versus the linear (A) coefficient (1) for all the second order fits to the SRA data of Figure 3. The straight line is a power law least -squares fitted to all the data. The straight line with dots is power law least-squares fitted to the data for which A < 40. The dashed curve is a straight line least-squares fitted to the data for which A < 40. The dotted straight line is a power law least-squares fitted to the three values (+) from the Voronovich and Zavorotny (2001) Ku-band theoretical analysis.

IMPACT/APPLICATIONS

The SRA provided the first comprehensive, quantified measurements of the directional wave spectrum spatial variation in the vicinity of hurricanes. The data impact all assessments of air/sea interaction in a hurricane environment and serve to validate wave models. The ability to examine the structure of individual waves and wave groups is important for assessing viability of marine structures.

RELATED PROJECTS

All hurricane components of ONR CBLAST.

REFERENCES

Moon, Il-Ju, Isaac Ginis, Tetsu Hara, Hendrik L. Tolman, C. W. Wright and E. J. Walsh, 2003: Numerical simulation of sea surface directional wave spectra under hurricane wind forcing, J. Phys. Oceanogr., 33, 1680-1706.

Plant, W. J., 1982: A relationship between wind stress and wave slope, J. Geophys. Res., 87, 1961-1967.

Walsh, E. J., D. W. Hancock, D. E. Hines, R. N. Swift, and J. F. Scott, 1985: Directional wave spectra measured with the surface contour radar, J. Phys. Oceanogr., 15, 566-592.

Walsh, E. J., D. W. Hancock, D. E. Hines, R. N. Swift, and J. F. Scott, 1989: An observation of the directional wave spectrum evolution from shoreline to fully developed, J. Phys. Oceanogr., 19, 670-690.

Walsh, E. J., L. K. Shay, H. C. Graber, A. Guillaume, D. Vandemark, D. E. Hines, R. N. Swift, and J. F. Scott, 1996: Observations of surface wave-current interaction during SWADE, The Global Atmosphere and Ocean System, 5, 99-124.

Walsh, E. J., C. W. Wright, D. Vandemark, W. B. Krabill, A. W. Garcia, S. H. Houston, S. T. Murillo, M. D. Powell, P. G. Black, F. D. Marks, 2002: Hurricane directional wave spectrum spatial variation at landfall, J. Phys. Oceanogr., 32, 1667-1684.

Wright, C. W., E. J. Walsh, D. Vandemark, W. B. Krabill, A. Garcia, S. H. Houston, M. D. Powell, P. G. Black, and F. D. Marks, 2001: Hurricane directional wave spectrum spatial variation in the open ocean, J. Phys. Oceanogr., 31, 2472-2488.

Voronovich, A. G., and V. U. Zavorotny, 2001: Theoretical model for scattering of radar signals in Ku- and C-bands from a rough sea surface with breaking waves. Waves in Random Media, 11, 247–269.

PUBLICATIONS

Black, P. G., E. A. D’Asaro, W. M. Drennan, J. R. French, P. P. Niiler, T. B. Sanford, E. J. Terrill, E. J. Walsh, J. A. Zhang, 2007: Air-Sea Exchange in Hurricanes: Synthesis of Observations from the Coupled Boundary Layer Air-Sea Transfer Experiment, Bull. Am. Met. Soc., 88, 357-374.

Chen, S. S., J. F. Price, W. Zhao, M. A. Donelan, E. J. Walsh, 2007: The CBLAST-Hurricane Program and the Next-Generation Fully Coupled Atmosphere-Wave-Ocean Models for Hurricane Research and Prediction, Bull. Am. Met. Soc., 88, 311-317.

Walsh, E. J., M. L. Banner, C. W. Wright, D. C. Vandemark, B. Chapron, J. Jensen, and S. Lee, 2008: The Southern Ocean Waves Experiment, Part III, Sea Surface Slope Statistics and Near Nadir Remote Sensing, J. Phys. Oceanogr., [in press, refereed].

Yalin Fan, Isaac Ginis, Tetsu Hara, C. W. Wright and E. J. Walsh, 2007: Numerical simulations and observations of surface wave fields under an extreme tropical cyclone, Chapter IV of “Effects of Surface Waves on Air-Sea Momentum and Energy Fluxes and Ocean Response to Hurricanes,” Yalin Fan Ph.D. dissertation, Graduate School of Oceanography, University of Rhode Island, peer-reviewed paper in preparation.